

6
9
2

V393
.R46

97

#2

MIT LIBRARIES



3 9080 02754 0936

NAVY DEPARTMENT

THE DAVID W. TAYLOR MODEL BASIN

Washington 7, D. C.



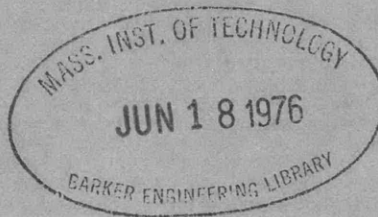
A SIX-COMPONENT DYNAMOMETER FOR THE MEASUREMENT OF FORCES AND MOMENTS ON MODELS OF SHIP APPENDAGES

BY

PHILLIP EISENBERG, MORRIS S. MACOVSKY, AND WALTER L. STRACKE

NE 051-427

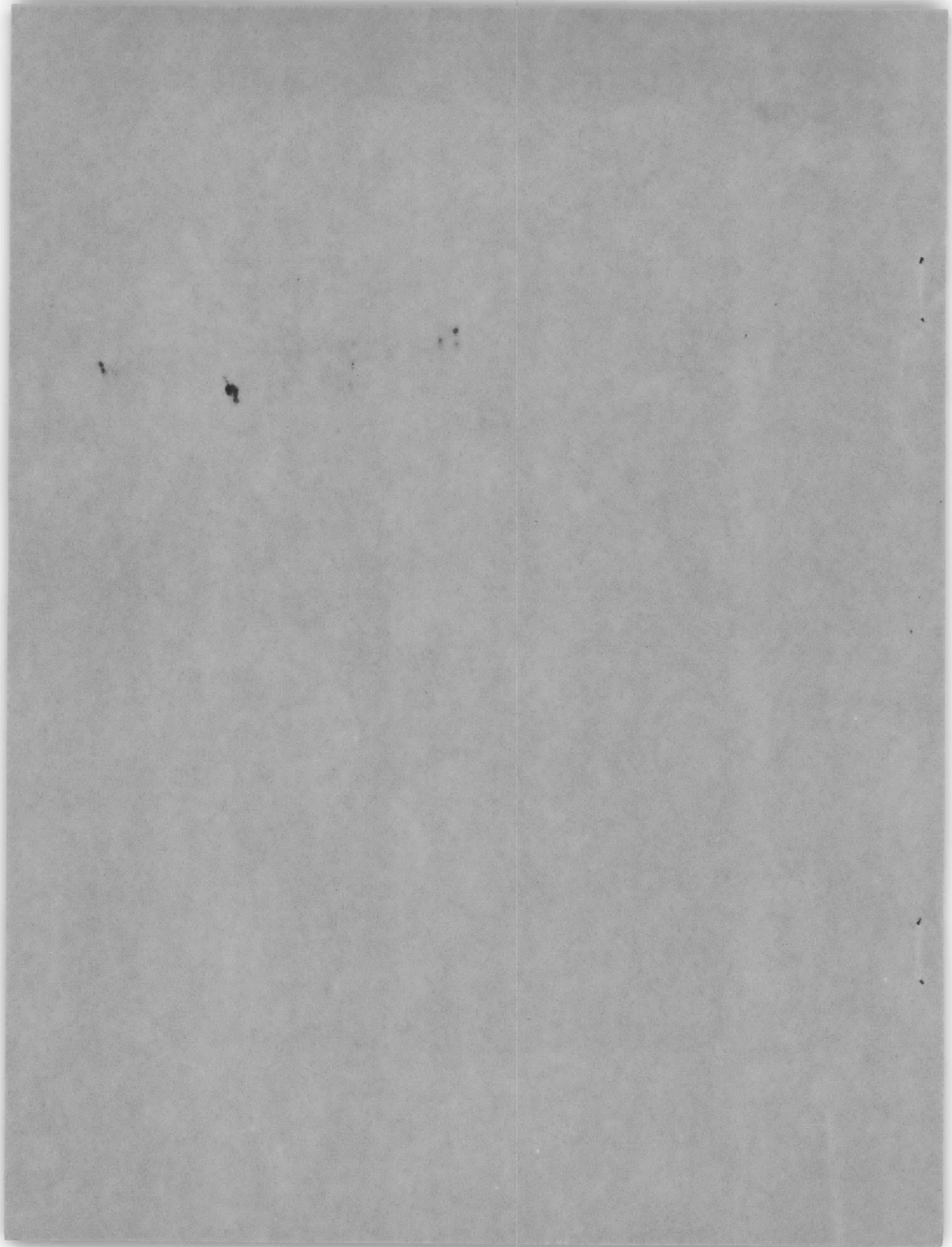
SRD 77/46



MAY 1949

REPORT 692

013349



INITIAL DISTRIBUTION

Copies

12 Chief, BuShips, Project Records (Code 362), for distribution:
3 Project Records
2 Sonar (Code 940)
2 Research (Code 330)
1 Model Basin Liaison (Code 422)
1 Applied Science (Code 370)
2 Preliminary Design (Code 420)
1 Submarines (Code 515)

2 Chief of Naval Research, c/o Science and Technology Project,
Library of Congress

2 Director, U.S. Naval Research Laboratory, Sound Division (Code 444)

2 Commander, Boston Naval Shipyard, Boston 29, Mass.

2 Commander, Portsmouth Naval Shipyard, Portsmouth, N.H.

1 Submarine Signal Company, 160 Washington St., North Boston, Mass.

1 Edo Corporation, College Point, Long Island, New York

2 Director, U.S. Navy Electronics Laboratory, Dome and Transducer
Group, San Diego 52, Calif.

1 Commander, Naval Ordnance Laboratory, White Oak, Silver Spring,
Md.

1 Director, Ordnance Research Laboratory, Pennsylvania State
College, State College, Pa.

1 Chief of the Bureau of Ordnance (Code Re6)

1 Dr. V.L. Streeter, Illinois Institute of Technology, 3300 Federal
St., Chicago 16, Ill.

1 Dr. J.W. Daily, Massachusetts Institute of Technology, Cambridge,
Mass.

1 Experimental Towing Tank, Stevens Institute of Technology, 711
Hudson St., Hoboken, N.J.

1 Hydraulic Laboratory, Newport News Shipbuilding and Dry Dock
Company, Newport News, Va.

1 Iowa Institute of Hydraulic Research, State University of Iowa,
Iowa City, Iowa

1 Hydrodynamics Laboratory, California Institute of Technology,
Pasadena 4, Calif.

1 Saint Anthony Falls Hydraulic Laboratory, University of Minnesota,
Minneapolis 14, Minnesota

1 Hydraulic Laboratory, National Bureau of Standards, Washington,
D.C.

A SIX-COMPONENT DYNAMOMETER FOR THE MEASUREMENT OF FORCES AND
MOMENTS ON MODELS OF SHIP APPENDAGES

by

Phillip Eisenberg, Morris S. Macovsky, and Walter L. Stracke

INTRODUCTION

With the development of retractable sonar domes, the David Taylor Model Basin has been receiving an increasing number of requests for tests to determine the forces and moments on such domes for use in the design of the retracting mechanisms. Although several models have been tested with dynamometer arrangements adapted for the specific components required, the need for an instrument to furnish the forces and moments about the principal axes for any model submitted became apparent in 1947. As a result the design of a six-component dynamometer, which is quickly adapted to any type of sonar dome model and for either translational or rotational retraction, was undertaken. With the completion of the dynamometer these tests can now be made in a routine manner. In addition to its use with sonar-dome models, the dynamometer was designed to be used with models of other ships' appendages, such as rudders and propeller-shaft struts.

The design of the dynamometer and housing combination was based on requirements that the arrangement be easily launched for tests in the model basin, that it be towed under the centerline of the towing carriage, and that changes in the depth and orientation of the model be made from above the water surface. The intended position of the arrangement below the towing carriage was such as to make remote recording of data desirable.

It is the purpose of this report to describe the development and use of the dynamometer and the methods of deriving the forces and moments from the dynamometer data for fixed and body axes. Since the arrangement will be used first with sonar domes, this application is emphasized; however, the application to other types of models will be similar. A note is included on stimulation of free-stream turbulence when testing models that can be accommodated by the dynamometer.

DESCRIPTION AND DEVELOPMENT OF THE
SIX-COMPONENT DYNAMOMETER

The dynamometer is essentially a triangular platform to which the model is rigidly secured and which is supported only by six force elements or dynamometers; see Figure 1. On the basis of previous experience with such

| | | |
|------------------------------|-----------------------------------|----------------------------|
| a - Forward Lift Dynamometer | f - Inner (Threaded) Spindle | n - Pin-Locking Bolts |
| a' - After Lift Dynamometers | g - Handwheel (Vertical Position) | o - Cylinder (Fixed) |
| b - Forward Yaw Force | h - Vertical Position Lock | p - Bottom (Contour) Plate |
| b' - After Yaw Force | i - Yaw Position Lock | q - Model |
| c - Drag Dynamometer | j - Yaw-Positioning Arm | r - Dynamometer Frame |
| d - Spider | k - Cylinder (Rotating) | s - Faired Housing |
| e - Outer Spindle | l - Clamp | t - Spray Shields |
| | m - Pin | u - Turbulence Rod |

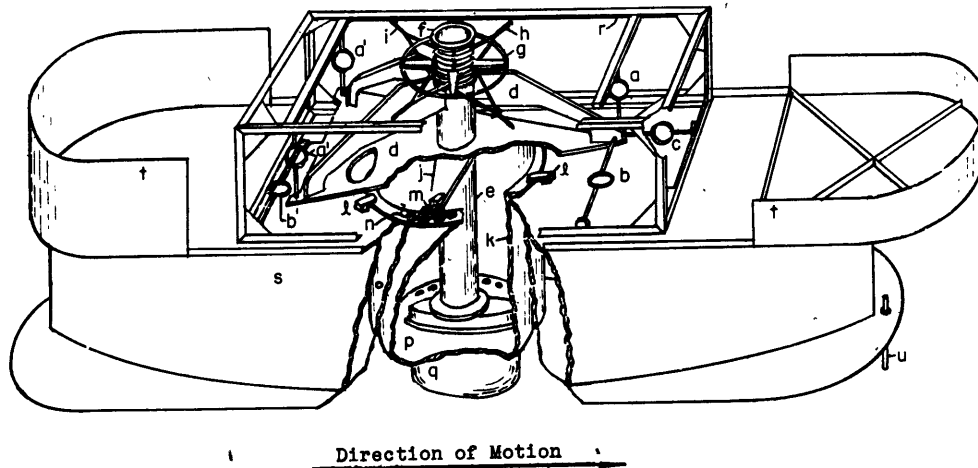


Figure 1 - Sketch of Six-Component Dynamometer

combinations ^{1, 2}, steel rings to which are cemented resistance-wire strain gages, are used as force elements. The rings are in turn supported by a rigid frame which is otherwise independent of the dynamometer and the model. These rings and the electric circuits used with the strain gages are discussed in a subsequent section. The design loads for the supporting structure of the dynamometer are based on allowable limits of deformation rather than of stress. The maximum loads are: drag, 100 lb; lift or vertical force, 200 lb; and side or cross force, 120 lb. The accuracy and resolution desired for any particular model may be obtained by choosing a set of rings designed for the actual maximum loads expected. For tests of sonar-dome models as well as other ship appendages the dynamometer assembly is used with the faired housing shown in Figure 1 (see also Figures 2 and 3). The housing shields the submerged parts of the dynamometer and simulates the ship's bottom in the vicinity of the appendage insofar as the wall effect is concerned.*

The triangular dynamometer platform is supported at its vertices by three horizontal rings for carrying the drag and side forces and three vertical rings for carrying the vertical forces. The methods of deriving the forces and moments are discussed in another part of this report. Since each ring must carry tensile and compressive forces, self-aligning ball bearings

¹ All references will be found on page 16.

* To simulate the actual boundary layer of the ship, auxiliary means must be used.

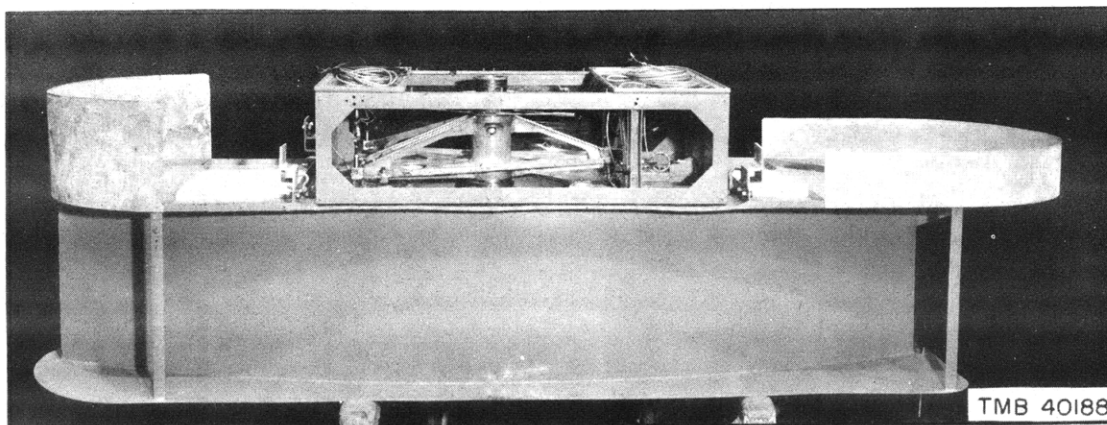


Figure 2 - The Six-Component Dynamometer and Faired Housing Bolted Together and Viewed from the Starboard Side

The wooden hatches cover watertight holes in which weights may be placed for ballasting to the proper water lines. The angle indicator may be seen on the spindle; a vernier is also on the faired housing. The turbulence rod is shown installed.

rather than flexure plates or rods were considered for use throughout the dynamometer. Tests to determine the starting friction of ball bearings indicated that the friction is so small as to be extremely difficult to measure; moreover, the towing carriage vibration was considered sufficient to overcome any friction forces not measurable. Consequently, ball-bearings were used for the ring-dynamometer reactions.

The dynamometer platform is part of a spider which also supports a spindle to which the model is attached. The spindle consists essentially of three concentric cylinders, the outer cylinder remaining fixed to the spider. The innermost cylinder holds the model and is threaded for raising or lowering by turning a collar. The two inner cylinders are keyed together to prevent relative rotation. The pitch of the threads is such that one complete revolution of the handwheel raises or lowers the model 1/2-in. These two cylinders are clamped together with the vertical position lock, Figure 1, and may rotate as a unit within the outer, fixed cylinder for changing the angles of yaw. The entire assembly is locked together with the yaw position lock. An angle indicator calibrated in degrees is inscribed on the middle cylinder and is viewed through a window in the outermost cylinder, Figure 2. The spider assembly, when not in use, can be locked in place by means of lock nuts situated at the vertices of the platform.

The faired housing is a symmetrical, circular-arc fairing 10 ft long and 2 ft wide at the maximum section, with a surface plate which has an overhang of 14 in. at the bow. Except for the center section the housing is

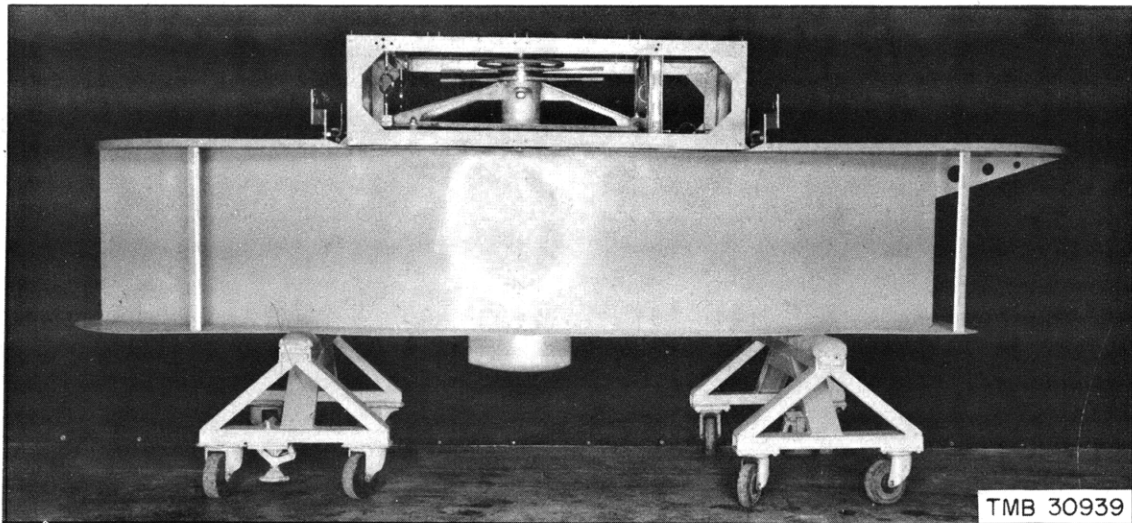


Figure 3 - The Six-Component Dynamometer and Paired Housing Showing the Position of a Typical Model

The spray shields are removed in this photograph.

watertight and has sufficient reserve buoyancy so that the entire dynamometer and housing assembly can be floated into position below the towing carriage. The housing is statically unstable in roll, and care must be taken when launching and floating into position. However, there is no difficulty after it has been bolted to the towing carriage. The top of the housing has open holds, so that weights may be added for ballasting. In the normal operating position, the bottom of the housing is 18 in. below the water line. The position of a typical model is shown in Figure 3.

At the center of the housing are two large concentric cylinders, the outer one being fixed to the housing. The inner cylinder can rotate with the dynamometer spindle and is fitted with a plate at the bottom which is flush with the bottom of the housing. This plate is made with an opening the shape of the model but with sufficient clearance so that the model does not touch when loaded. For models that must be retracted, this plate is the only part of the dynamometer which must be replaced for each different-shaped model. To maintain the relative orientation of the plate and model during a change in the yaw angle the housing cylinder is locked with a pin to the yaw-positioning arm which is fixed to the rotating cylinder of the dynamometer spider. (For rudder models, it is clear that the housing cylinder need not be rotated.) When the proper yaw angle has been set, the housing cylinder is clamped to the housing, the yaw position lock on the spider is set, and the yaw-positioning arm released from the housing by pulling the pin; see Figure 1. To increase the accuracy of setting the yaw angles, a vernier has been placed on the

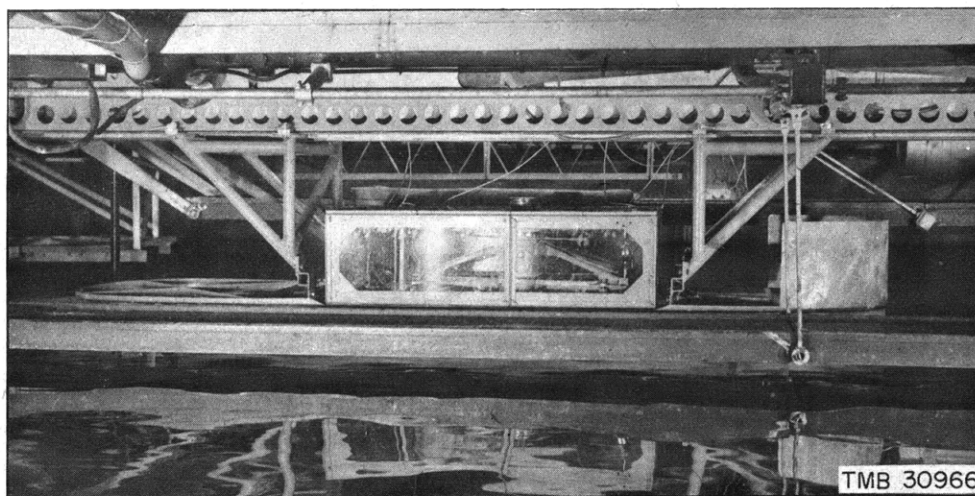


Figure 4 - The Dynamometer and Faired Housing Viewed from the Portside Showing the Method of Attachment to the Towing Carriage of the Deep Model Basin

The forward spray shield is removed. The lucite spray panels are shown installed on the dynamometer frame.

periphery of the large housing cylinder for setting angles in increments of 0.1° . It has also been found desirable to lock the spindle to the housing when setting the vertical position of the model. It is clear that the arrangement of dynamometer and housing is such that all changes in height and yaw may be made entirely above the water surface.*

The dynamometer and housing assembly is secured to the towing carriage in the manner shown in Figure 4. The large fore and aft brackets are bolted to the housing through the small offset hangers. Two sets of hangers are available, one set being the welded steel type shown in Figures 2 and 4. The other set is of the rubber-steel sandwich type for use in filtering out low-frequency carriage vibrations which may make it difficult to obtain small readings from the strain gages. These hangers are shown in Figure 3. Because of the large deflections that can result when using the latter type and which are produced by the lift developed on the bottom plate of the housing, it is recommended that these hangers be used only for tests that may be made at low speeds. In general, the first type can be used for most tests since the forced vibrations are of high frequency and small amplitude and do not impose any difficulties in obtaining readings of the magnitudes that will ordinarily be encountered. These were used throughout the tests reported herein.

* Additional attachments to the dynamometer spindle are available for simulating rotational retraction while using the various parts just as described herein. In this case, raising the threaded spindle rotates the model about a fixed point instead of raising or lowering the entire model.

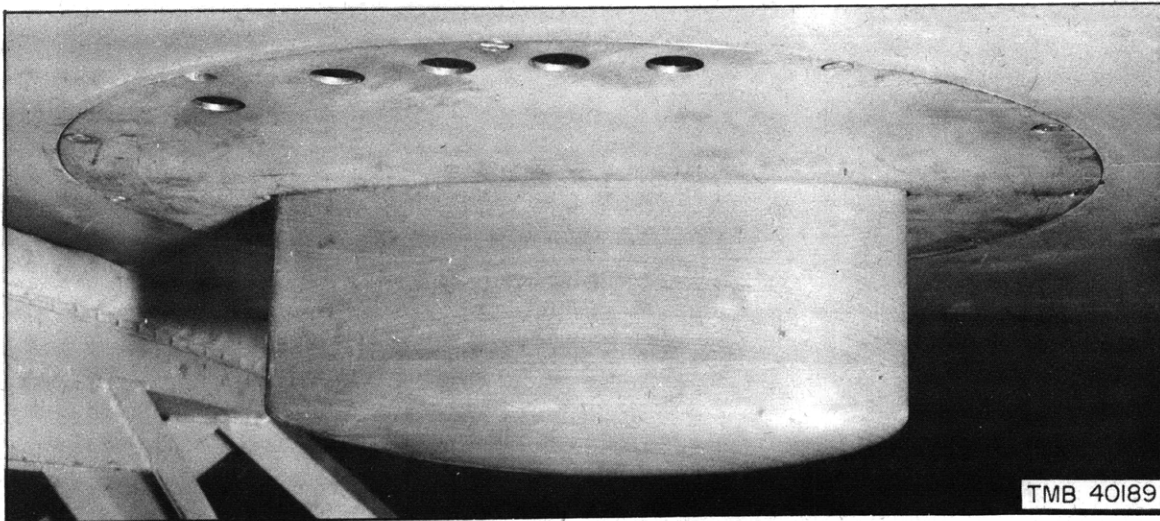


Figure 5 - View of a Model Taken from the Starboard Side and Below the Faired Housing and Showing the Flooding Holes

Exploratory tests of the system showed very large wave making by the housing. Consequently, a velocity survey was made in the region that would be occupied by the model in order to check the adequacy of the bottom plate of the housing in masking surface disturbances. It was found that despite the large surface disturbances, the velocities at the test section were well within 0.5 percent of the carriage speed--an accuracy better than that for any other measurement. The recommended maximum towing speed for the housing is 13 knots.

It was also found during the first tests with a model that the water in the housing cylinder was drawn out through the gap* between model and bottom plate during the accelerating portion of a run. When the steady part of the run was reached, a pressure difference remained across the bottom plate because of the resistance to flow through the gap. Since it took several seconds for equilibrium to be again reached, large differences from the steady-state vertical force on the model could be observed. To eliminate the possibility of errors resulting from taking readings too soon, and to assist the establishment of equilibrium conditions, several holes were drilled near the periphery of the bottom plate of the cylinder, Figure 5, on either side of the model. After these holes were drilled, tests were made to determine the influence on the model forces of the pressure relief and slight circulation within the cylinder resulting from the presence of the holes. Since no measurable difference could be observed in the forces on the model with and without these

* The gap was 0.20 in. with a model 15 in. long and 3 in. wide at the maximum section.

flooding holes in the plate, and since equilibrium conditions were established rapidly as a result of this modification, the flooding holes are recommended for all tests. Although ten 1-in. holes were used in the present tests, it is considered that six holes are sufficient.

DERIVATION OF FORCES AND MOMENTS FROM DYNAMOMETER DATA

In deriving the forces and moments from dynamometer data, the convention of Figure 6 is adopted. (Where applicable, the nomenclature of Reference (3) is used herein.) The direction of the arrows are the positive directions for the axes and components. The origin of coordinates is taken at the point O fixed in the model. The "fixed" axes (x_0 , y_0 , z_0) are oriented with the positive x_0 -direction in the direction of motion, the positive y_0 -direction to starboard, and the positive z_0 -direction downward. The body axes (x , y , z) are fixed in the model and are oriented with respect to the fixed axes by a simple rotation about z_0 through the angle of yaw β . The drag D, cross force C, and lift L refer to the fixed axes; the corresponding forces referred to the body axes are X, Y, and Z.

The positive direction of the drag force D is the negative x_0 -direction; and the positive direction of the cross force C is in the negative y_0 -direction. The positive direction of the vertical force L is in the positive z_0 -direction. The body forces X, Y, and Z are taken as positive in the positive direction of the axes. The pitching moments M_0 and M are taken as positive in the clockwise direction when viewed from port to starboard (i.e., in the positive y_0 - and y-directions); the rolling moments K_0 and K are taken positive in the clockwise direction when viewed from aft to forward (i.e., in the positive x_0 - and x-directions); the yawing moments N_0 and N are taken positive in the clockwise direction when viewed from the negative to the positive z_0 - and z-directions. The forces F on the dynamometer are taken as positive when they put the rings in tension.

From Figure 6, the scalar values of the forces and moments relative to the fixed axes (x_0 , y_0 , z_0) are given by

$$D = F_1 \quad [1]$$

$$L = F_2 + F_3 + F_4 \quad [2]$$

$$C = F_5 + F_6 \quad [3]$$

$$M_0 = D_c - [L - 2(F_3 + F_4)]a \quad [4]$$

$$N_0 = (F_5 - F_6)a = (C - 2F_6)a \quad [5]$$

$$K_0 = (F_4 - F_3)b - Cc \quad [6]$$

The forces and moments referred to body axes are computed from the following transformations:

$$X = -D \cos \beta - C \sin \beta \quad [7]$$

$$Y = D \sin \beta - C \cos \beta \quad [8]$$

$$Z = L \quad [9]$$

$$M = M_0 \cos \beta - K_0 \sin \beta \quad [10]$$

$$K = M_0 \sin \beta + K_0 \cos \beta \quad [11]$$

$$N = N_0 \quad [12]$$

The arrangement of the strain-gage circuits for simplifying some of the computations and improving the accuracy of values obtained from differences of dynamometer readings is described in the following section.

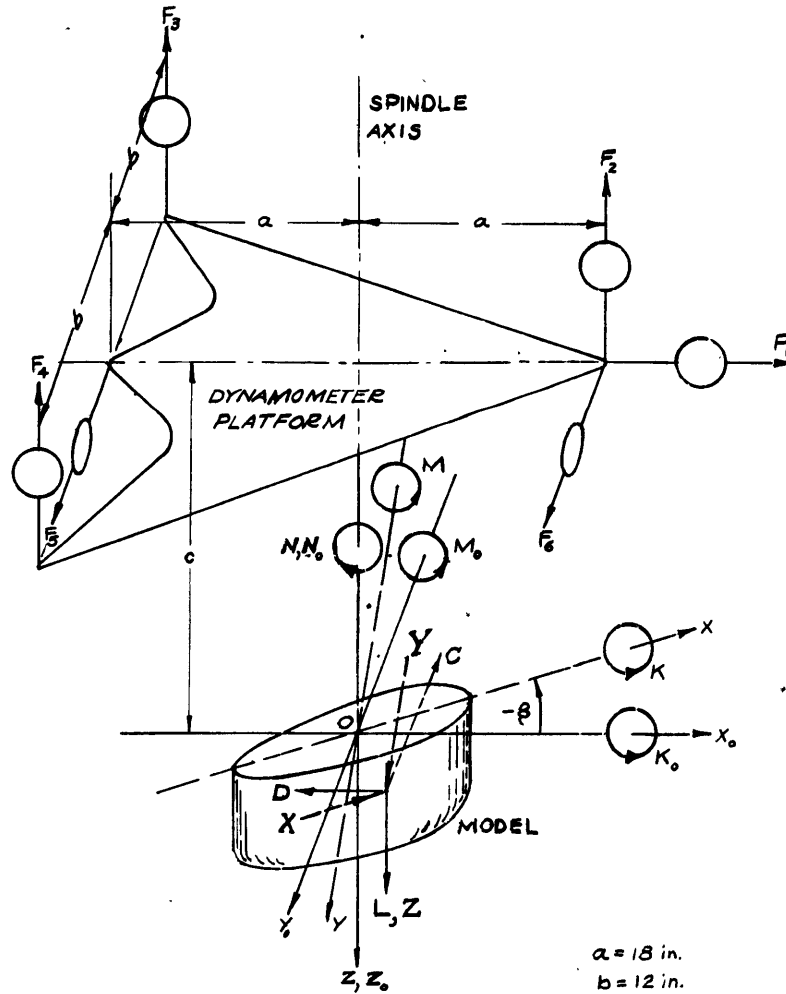
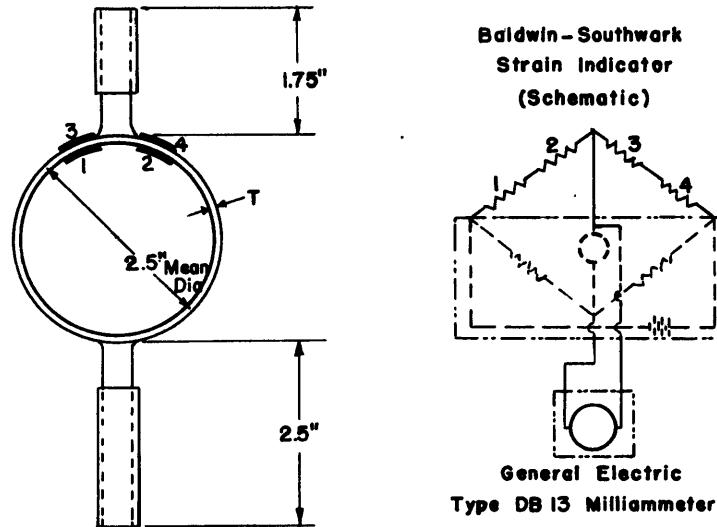


Figure 6 - Force and Moment Convention for Dynamometer and Model

STRAIN GAGE CIRCUITS AND METHOD OF RECORDING

In the present application of resistance-wire strain gages, four Type A-7 Baldwin-Southwark strain elements are cemented* to each ring at approximately the position of maximum strain, Figure 7. The gages are arranged so that when one pair is in tension, the other pair is in compression. Each pair is connected in series and positioned in a bridge circuit so that strains of opposite sign are additive, thus providing greater sensitivity in the dynamometer. That this will occur is readily evident from the schematic circuit diagram of Figure 7. For most models, the SR-4 Type K Baldwin-Southwark strain indicator is sufficient for recording the resultant strain values due to the component forces and moments. For many models, however, the forces may



**RING DYNAMOMETER
CHARACTERISTICS**

| Ring No. | Thickness T in. | Maximum Design load lb | Measured Sensitivity μ in./in. |
|----------------|-----------------|------------------------|------------------------------------|
| F ₁ | 0.070 | 81 | 49.7 |
| F ₂ | 0.090 | 134 | 33.2 |
| F ₃ | 0.130 | 280 | 15.2 |
| F ₄ | 0.130 | 280 | 15.4 |
| F ₅ | 0.070 | 81 | 59.0 |
| F ₆ | 0.070 | 81 | 57.5 |

Figure 7 - Ring Dynamometer Characteristics and Schematic Wiring Diagram

* Gages are mounted on the rings with DuPont Cement, and oven dried according to the temperature schedule prescribed by the Baldwin-Southwark Corporation.

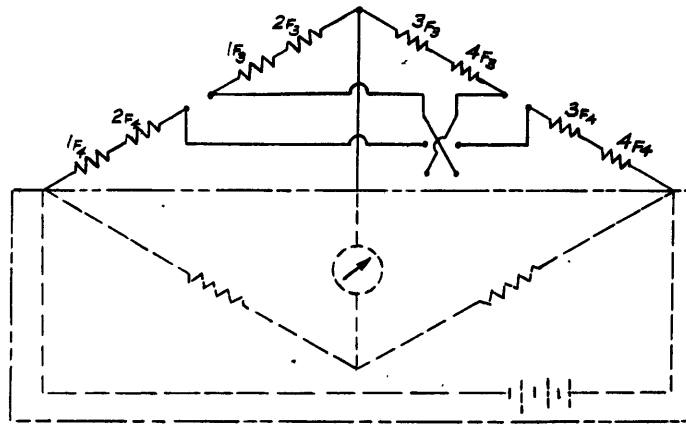


Figure 8 - Schematic Wiring Diagram of Ring Dynamometers F_3 and F_4 for Reading $(F_4 + F_3)$ and $(F_4 - F_3)$ Directly

show such high amplitude oscillations that it is advisable to use a highly damped meter for recording. As indicated in Figure 7, a General Electric Type DB-13 milliammeter, which has appreciable mechanical damping, placed in parallel with the galvanometer of the SR-4 indicator, is suitable.

For most models that will be tested with the dynamometer, the differences between the forces F_3 and F_4 will be small although the forces themselves may be large. This situation may also occur for F_5 and F_6 . Equations [2] through [6] indicate that only the sum and difference of these forces are required and not the individual values of each force. As a result, to improve the accuracy of the measured values, the gages on these four rings may be wired as illustrated in Figure 8. It is clear that the sensitivities of the gages must be very nearly the same for this circuit to be used.* Although this circuit results in a considerable reduction in sensitivity of the combination, nevertheless the increased accuracy in the readings and the reduction in oscillations will usually overcompensate the loss in sensitivity.

CALIBRATION OF THE RINGS AND DYNAMOMETER

A complete calibration of the six-component dynamometer consists in determining the sensitivities of the component rings individually both before and after they are assembled on the dynamometer frame. To obtain the former

*To match the sensitivities of gages will usually require several trials. For the exploratory tests with the dynamometer, the circuit of Figure 8 was used only for gages F_3 and F_4 , which were matched within 1.3 percent (see table of Figure 7).

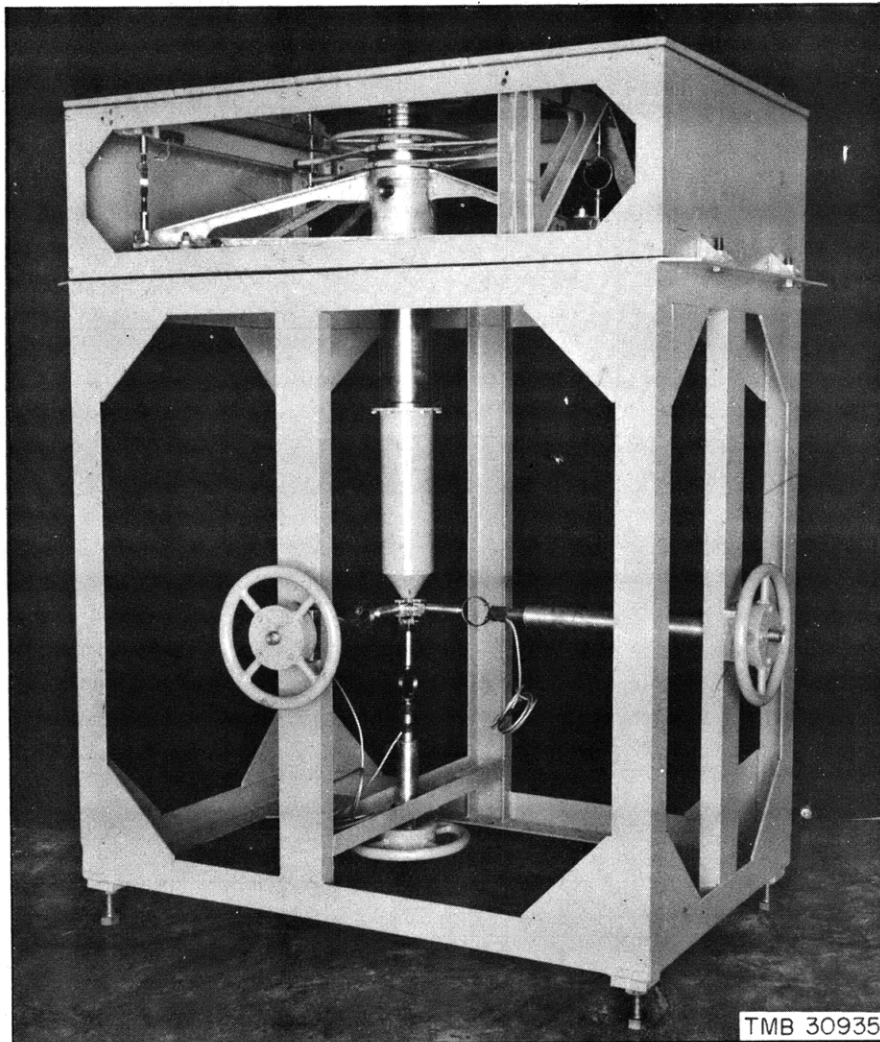


Figure 9 - Calibrator and Six-Component Dynamometer
Assembled for Normal Calibration

calibration it is sufficient to hang each ring suitably in a vertical position and to add known weights to a scale pan suspended from the ring. On the other hand, to obtain the calibration of the assembled system of rings, it is necessary to provide a suitable means of applying known loads to the system at a point coincident with that at which actual test loads are applied. The calibration stand of Figure 9 was constructed for this purpose.

Each ring of the six-component dynamometer was suspended vertically, and fitted with a scale pan at its lower end. Prior to actual calibration,

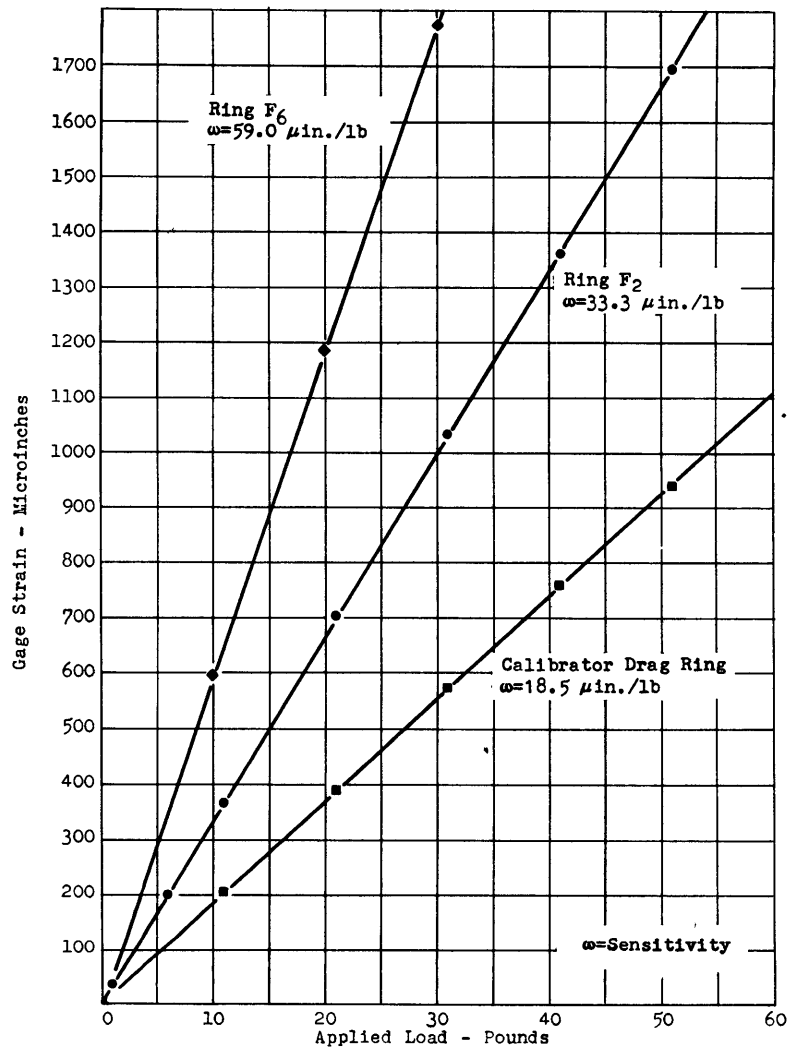


Figure 10 - Typical Ring-Dynamometer Calibrations

prestressing loads, in the order of magnitude of the maximum operating load* for each ring, were applied to the pan for a period of approximately 30 minutes. Following the period of prestressing, the scale pan was loaded in convenient steps up to the maximum load and unloaded in similar steps in order to detect any hysteresis. In each instance the resulting calibration curves were linear without hysteresis, as exemplified in Figure 10. Obviously this

* Maximum operating loads are defined as those loads which produce 2000 $\mu\text{in./in.}$ of strain in any wire strain gage element on the ring. Actually strains of 3000 $\mu\text{in./in.}$ can be applied safely. Ring thicknesses were chosen such that maximum operating loads are approximately one half maximum design loads for the rings (Figure 7), which were made from U.S. Navy Specification 49S-2 Alloy 2 steel (yield point $105 \times 10^3 \text{ lb/in.}^2$; Young's modulus $30 \times 10^6 \text{ lb/in.}^2$).

technique calibrated the rings in tension only. The validity of the calibrations for compression was later proved by the calibration of the assembled system on the calibration stand.

The calibration stand shown in Figure 9 provides a method of simulating test loading of the assembled six-component dynamometer. The stand consists of a steel framework upon which the dynamometer frame can be bolted. The calibration standards consist of three ring dynamometers wired as were the six rings of Figure 7. These rings have a mean diameter of 2 1/2 in. and vary in thickness depending on the expected maximum loading* of the particular component to be simulated. Each ring is silver-soldered to two steel rods 1 in. in diameter; one end of the assembled unit is threaded and the other fitted with a pivot block. The threaded end of each unit is passed through a tapped handwheel mounted in gimbal rings and secured to the calibrator strut, which is bolted to the dynamometer spindle. The rings when mounted form a mutually perpendicular system whose origin during calibration should lie on the axis of the dynamometer spindle and whose directions should be parallel to the force axes of the six-component dynamometer. With the dynamometer properly mounted on the stand, loads applied to the calibrator rings by turns of the handwheels should be reflected, without loss, in the six-component dynamometer rings.

The calibrator standard rings were calibrated in the same manner as each of the six dynamometer rings. A sample calibration of the drag standard is given in Figure 10.

Proper alignment of the dynamometer axes relative to the calibrator axes was accomplished by applying the calibrator standards individually. At first only the calibrator drag ring was pinned to the spindle. A known drag load was applied to the system, and the six-component dynamometer was reoriented on the stand until the drag ring, F_1 , reproduced the applied load. It was observed that in this position the applied load was reproduced for loading in either tension or compression, proving that the previous tension calibration of the calibrator and of F_1 held for compression as well. This procedure was repeated, using only the cross-force calibrator. The dynamometer was finally positioned so that drag and cross force applied simultaneously by the calibrator were reproduced by the dynamometer. The vertical-force axes of the calibrator and dynamometer were now expected to coincide. Application of only vertical force by the calibrator proved this to be so.

An overall calibration of the dynamometer was finally conducted by applying all of the calibrator forces simultaneously and randomly over the full range of the six-component dynamometer. An accuracy of better than 2

* See footnote on page 12.

percent was observed in the reproduction of the applied loads for either tensile or compressive loading.

Finally, as a check upon the accuracy of the instrument, the drag of a model was measured both by the six-component dynamometer and by the dynamometer of the towing carriage. In both instances the model was mounted in the housing, as shown in Figure 3. The difference between the two measurements was less than 3 percent.

NOTE ON TURBULENCE STIMULATION WHEN USING THE FAIRED HOUSING

In general, the models that will be tested with the dynamometer are of comparatively small scale so that care must be taken to ensure that tests are made at Reynolds numbers beyond the transition from laminar to turbulent flow in the boundary layer--a condition necessary in the prediction of full-scale performance from model data. It was of interest, therefore, to determine whether artificial means must be used to stimulate transition within the range of Reynolds numbers obtainable when using the faired housing.

For this purpose, tests were made on a strut form of low-aspect ratio with and without stimulation of free-stream turbulence. Stimulation was attempted by using a rod fixed upstream of the model; see Figures 1 and 2. The selection of the turbulence rod was made on the basis of the results reported by Townsend⁴ and Hall⁵. A rod $3/8$ in. in diameter was placed 144 rod diameters ahead of the model. The results of References 4 and 5 indicate that for this configuration and for the Reynolds numbers of the rod (up to 5.7×10^4) the turbulence is nearly stabilized but that the intensity is still fairly high, with maximum values somewhat in excess of 2.5 percent of the free-stream velocity for all components. In addition, at the position of the model the average velocity across the wake of the rod is only 5 percent less than the free-stream velocity.

The effects of stimulation were examined on the basis of the dependence of the drag coefficients of the model on the Reynolds number of the model. The results are shown in Figure 11. The coefficients obtained with the turbulence rod show the apparently anomalous result that there was actually a smaller degree of turbulence in the stream when the tests were made with the rod and that transition was somewhat delayed. However, this can be explained by the following observations. The tests made without the rod were begun only after a number of preliminary runs in the model basin, so that the water had been considerably disturbed by the large housing before the tests were actually begun. On the other hand, the tests with the rod were made after the basin had been settling for about an hour. The values of the coefficients for this condition at Reynolds numbers below 7×10^5 were all obtained during the first run

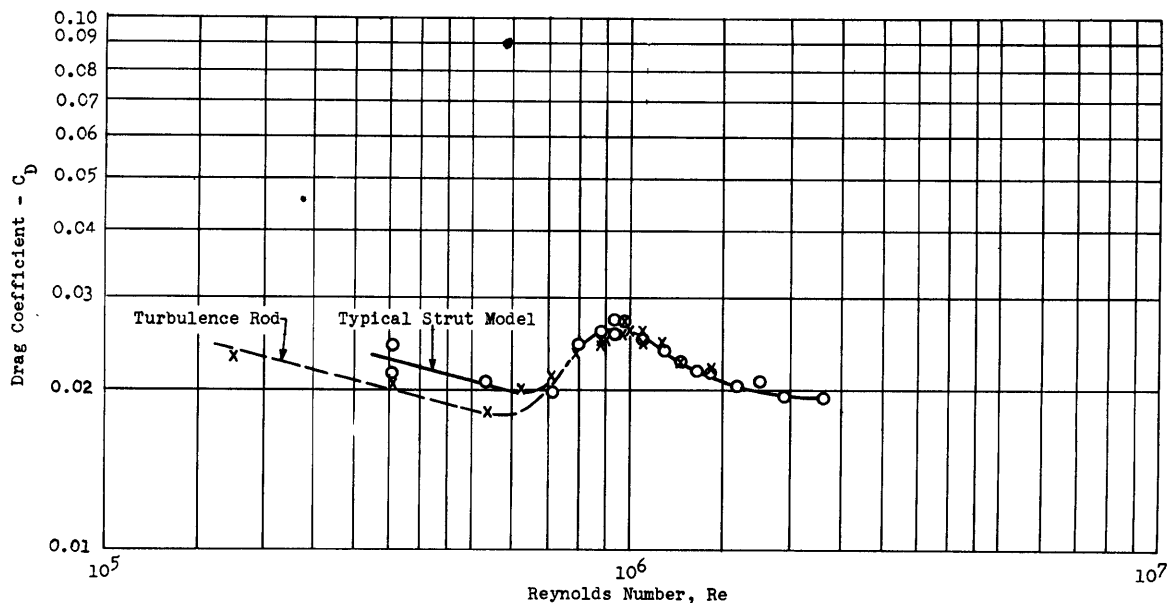


Figure 11 - Dependence of Force Coefficients on Reynolds Number for a Typical Strut Model

in the undisturbed water so that the model was influenced primarily by the rod. For the subsequent runs, the drag coefficients coincide with those obtained without the rod.

From these results, it may be concluded that a rod used as described herein is not as effective as several runs with the housing in stimulating free-stream turbulence. On the other hand, unpublished data--obtained in 1934 at the U.S. Experimental Model Basin by Thews and Landweber--on the drag of flat plates indicate that small rods at distances up to 10 diameters ahead of a model are apparently effective in inducing transition, although the actual mechanism is not clear. Transition was shown to have occurred at Reynolds numbers below 10^5 with a spacing of 10 diameters. For smaller spacings, however, transition was delayed to higher Reynolds numbers. In view of the present tests, it appears that there is an optimum spacing for such turbulence rods. As a result, it is recommended that, when the housing is used, several runs be made before making measurements. If further stimulation is required small rods near the model, crossed wires about 16 rod diameters ahead of the model², or the usual trip wires or sand strips may be used.

SUMMARY AND CONCLUDING REMARKS

The development, calibration, and operation of a six-component dynamometer for the measurement of forces and moments on models of ship appendages

has been described. The force-measuring elements are steel rings to which are cemented resistance-wire strain gages. When using the strain-gage circuits described herein, average dynamometer readings are obtained by individual operators. However, it is clear that continuous recording may be used if needed. Continuous recording may be of use in indicating the degree of instability of various forces, although such records must be interpreted with care because of the dependence of oscillating flows on Reynolds number.

Because of the comparatively small models that can be tested with the dynamometer, the question of turbulence stimulation has been considered insofar as initial turbulence in the free stream is concerned. From the experiments with a turbulence rod, it was concluded that the faired housing is just as effective in stimulating free-stream turbulence as a rod used in the manner described herein. On the other hand, a small rod placed about 10 diameters ahead of the model has been shown to induce early transition, although the actual mechanism is not clear. It was also shown in these earlier tests that smaller distances are not as effective as 10 diameters. Thus, it may be concluded that free-stream turbulence alone is not the primary factor in inducing transition and that there is an optimum position for rods used as stimulators.

PERSONNEL

The work described in this report, including the specifications for and the development of the dynamometer, was carried out by Phillip Eisenberg, Morris S. Macovsky, and Walter L. Stracke of the Hydromechanics Laboratory. The mechanical design of the dynamometer is the work of M. Cuniberti of the Engineering and Design Branch.

REFERENCES

- (1) "Model Tests to Determine the Forces on the Stern-Gate Operating Mechanism of the ARD12 Class of Floating Drydocks in Waves," by M. Gertler, TMB RESTRICTED Report R-310, Feb 1947.
- (2) "Determination of the Torque Required for Retracting the NRL 110-Inch Sonar Dome," by P. Eisenberg and M.S. Macovsky, TMB RESTRICTED Report R-358, Sept 1947.
- (3) "A Proposed Nomenclature for Treating the Motion of a Submerged Body through a Fluid," by L. Landweber and M.A. Abkowitz, TMB Report prepared for Committee on Nomenclature of the American Towing Tank Conference, second revision, Dec 1948.

(4) "Measurements in the Turbulent Wake of a Cylinder," by A.A. Townsend, Proc. Royal Soc. London, Ser. A, Vol. 190, pp. 551-561, Sept 1947.

(5) "Measurements of the Scale and Intensity of Turbulence," by A.A. Hall, (British) Aeronautical Research Committee, Reports and Memoranda 1842, Aug 1938.

RECEIVED
OCT 5 1954
DIRECTOR OF NAVAL MAT

MIT LIBRARIES

DUPL



3 9080 02754 0936

